Self-Organizing Recurrent Fuzzy Wavelet Neural Network-Based Mixed $\mathcal{H}_2/\mathcal{H}_\infty$ Adaptive Tracking Control for Uncertain Two-Axis Motion Control System

Fayez F. M. El-Sousy
Member, IEEE
Prince Sattam bin Abdulaziz University
College of Engineering, Electrical Engineering Department
Al-Kharj, Saudi Arabia
f.elsousy@psau.edu.sa

Khaled A. Abuhasel
Prince Sattam bin Abdulaziz University
College of Engineering, Mechanical Engineering Department
Al-Kharj, Saudi Arabia
k.abuhasel@psau.edu.sa

***Abstract*—In this paper, an intelligent adaptive tracking control system (IATCS) based on the mixed $\mathcal{H}_2/\mathcal{H}_\infty$ approach for achieving high precision performance of a two-axis motion control system is proposed. The two-axis motion control system is an X-Y table driven by two permanent-magnet linear synchronous motors (PMLSMs) servo drives. The proposed control scheme incorporates a mixed $\mathcal{H}_2/\mathcal{H}_\infty$ controller, a self-organizing recurrent fuzzy-wavelet-neural-network controller (SORFWNNC) and a robust controller. The SORFWNNC is used as the main tracking controller to adaptively estimate an unknown nonlinear dynamic function (UNDF) that includes the lumped parameter uncertainties, external disturbances, cross-coupled interference and frictional force. Furthermore, a robust controller is designed to deal with the approximation error, optimal parameter vectors and higher order terms in Taylor series. Besides, the mixed $\mathcal{H}_2/\mathcal{H}_\infty$ controller is designed such that the quadratic cost function is minimized and the worst case effect of the UNDF on the tracking error must be attenuated below a desired attenuation level. The online adaptive control laws are derived based on Lyapunov theorem and the mixed $\mathcal{H}_2/\mathcal{H}_\infty$ tracking performance so that the stability of the IATCS can be guaranteed. The experimental results confirm that the proposed IATCS grants robust performance and precise dynamic response to the reference contours regardless of external disturbances and parameter uncertainties.**

***Index Terms*—Fuzzy wavelet neural network, Lyapunov satiability theorem, mixed $\mathcal{H}_2/\mathcal{H}_\infty$ tracking performance, PMLSM, two-axis motion control system, X-Y table.**

I. INTRODUCTION

Nowadays, there is an increasing demand for modern precision positioning systems such as machine tools, micro-machining for semiconductor, microelectronics manufacturing equipment and optical pointing devices. These systems are often required to operate in high speed to yield high productivity [1], [2]. The development of a compact and high performance motion controller for the two-axis X-Y table of a computer numerical control (CNC) machine has been an important field in literatures [3]-[4]. The two-axis X-Y table system is usually subjected to unmodelled dynamics, external disturbances and the cross-axis coupling interferences, which often deteriorate the system performance during a machining process. With the recent advances of computer technologies, control theories and material technologies, the requirement for the performance of numerical control machine tools is increasing. Representative of the permanent magnet linear synchronous motor (PMLSM) X-Y table system, with its fast response and accurate positioning and high reliability has been widely used in aerospace, semiconductor and high-speed automated processing equipment. However, the PMLSM is greatly affected by force ripple, parameter variations and external load disturbances in the drive system. Moreover, the machine can exhibit cogging forces. Therefore, these parameter variation and dominant disturbances should be compensated to achieve high-speed/high-positioning precision control in PMLSM motion systems. There must adopt an effective control strategy to inhabit these disturbances for the control requirements of PMLSM [5]-[7].

Intelligent control techniques in much research have been developed to improve the performance of nonlinear systems and to deal with the nonlinearities and uncertainties using fuzzy logic, neural network, wavelet and/or the hybrid of them [8]–[10]. A fuzzy wavelet neural network (FWNN) is combined wavelet theory with fuzzy logic and NN that can bring the low-level learning, good computational capability of the WNNs into fuzzy system and also high-level humanlike IF-THEN rule thinking reasoning of fuzzy system into the WNNs. The synthesis of a fuzzy wavelet neural inference system includes the determination of the optimal definitions of the premise and the consequent part of fuzzy IF–THEN rules. The FWNNs consist of a set of rules and each rule contains a wavelet function in the consequent part of the rule. With the identification and control applications, some researchers [11]-[15] presented the FWNNs structures that used the gradient descent method to update/tune network parameters including wavelet parameters and weights.

The ever increasingly stringent performance requirements of two-axis motion control systems driven by PMLSMs have forced control researchers to look beyond traditional linear control theory for more advanced controllers. During the past decade, a mathematically rigorous adaptive control [16]-[18], sliding-mode control [19]-[21], robust control [22], intelligent control [23]-[26], for PMLSM drive systems has been developed achieving significant performance improvement in motion control applications. In addition, the intelligent control [27]-[31] for two-axis motion control system driven by PMLSM servo drives is also presented. Although different control strategies have been proposed to address the control design for the two-axis motion control systems, to the best of my knowledge, there are still no published research works to deal with the intelligent mixed $\mathcal{H}_2/\mathcal{H}_\infty$ adaptive tracking control problem for the two-axis motion control systems.

978-1-4799-8374-0/15/$31.00 © 2015 IEEE

The mixed control design is appealing for control engineers since it combines the merits of both the optimal control and the robust control. Mixed control problems for linear systems [32], [33] and nonlinear systems [34], [35] have been studied by many researchers. The $\mathcal{H}_2$ tracking design is related to minimizing the linear quadratic cost of tracking error and control input [32]. The $\mathcal{H}_\infty$ tracking design is related to attenuating the effect of the external disturbances. The main purpose of this type of control is to design an $\mathcal{H}_2$ optimal control for the worst-case external disturbance whose effect on system output must be attenuated below a desired value [34], [35] *i.e.*, to design an $\mathcal{H}_2$ optimal control under $\mathcal{H}_\infty$ disturbance attenuation constraint.

II. Preliminaries

A. Modeling of the Two-Axis X-Y Table Driven by PMLSMs

The mathematical modeling of the single-axis PMLSM in the synchronously rotating reference frame is described as follows [5]-[7].

$$V_{qs}^r = R_s i_{qs}^r + \frac{d}{dt}\lambda_{qs} + \omega_r \lambda_{ds} \tag{1}$$

$$V_{ds}^r = R_s i_{ds}^r + \frac{d}{dt}\lambda_{ds} - \omega_r \lambda_{qs} \tag{2}$$

$$\lambda_{qs} = L_{qs} i_{qs}^r \tag{3}$$

$$\lambda_{ds} = L_{ds} i_{ds}^r + \lambda_{PM} \tag{4}$$

$$\omega_r = (P/2)\omega \tag{5}$$

Substituting (3), (4) into (1), (2) will yield

$$V_{qs}^r = R_s i_{qs}^r + L_{qs}\frac{d}{dt} i_{qs}^r + \omega_r L_{ds} i_{ds}^r + \omega_r \lambda_{PM} \tag{6}$$

$$V_{ds}^r = R_s i_{ds}^r + L_{ds}\frac{d}{dt} i_{ds}^r - \omega_r L_{qs} i_{qs}^r \tag{7}$$

where V_{qs}, V_{ds}, i_{qs} and i_{ds} are the *d-q* axis armature voltages and currents respectively. R_s is the resistance of armature windings, L_{ds} and L_{qs} are the *d-q* axis inductances, and λ_{PM} is the permanent magnet flux linkage. ω_r, ω and P are electrical angular velocity, angular velocity of the mover and the number of primary poles, respectively. Moreover

$$\omega = (\pi/\tau_p)v \tag{8}$$

$$v_r = (P/2)v = 2\tau_p f_r \tag{9}$$

where v_r, v, f_r and τ_p are electrical linear velocity, mover linear velocity, frequency and the pole pitch, respectively.

The developed electromagnetic thrust can be expressed as:

$$F_e = \frac{3}{2}\cdot\frac{P}{2}\cdot\frac{\pi}{\tau_p}[\lambda_{ds} i_{qs}^r + (L_d - L_q) i_{ds}^r i_{qs}^r] \tag{10}$$

Then, using FOC and setting d-axis current as zero, the electromagnetic thrust is obtained as given in (11).

$$F_e = \frac{3}{2}\cdot\frac{P}{2}\cdot\frac{\pi}{\tau_p}\cdot\lambda_{PM} i_{qs}^r = K_f i_{qs}^r \tag{11}$$

$$K_f = \frac{3}{2}\cdot\frac{P}{2}\cdot\frac{\pi}{\tau_p}\cdot\lambda_{PM} \tag{12}$$

where K_f is the thrust constant and i_{qs}^r is the command of thrust current and F_e is the electromagnetic thrust.

The dynamic equation of the mover motion with the friction model included is given by:

$$F_e = M\frac{d}{dt}v + Dv + F_L + F_f(v) \tag{13}$$

where M is the total mass of the mover, D is the viscous friction and iron-loss coefficient; F_L and $F_f(v)$ are the external disturbance load force and the frictional force. Considering Coulomb friction, viscous friction and Stribeck effect, the friction force can be formulated as follows [6].

$$F_f(v) = F_C\,\mathrm{sgn}(v) + (F_S - F_C)e^{-(v/v_s)^2}\,\mathrm{sgn}(v) + K_v v \tag{14}$$

where F_C is the Coulomb friction, F_S is the static friction, v_s is the Stribeck velocity parameter, K_v is the coefficient of viscous friction and sgn(·) is a function. All the parameters in (13) are time varying.

B. Dynamic Analysis and Properties

The dynamic analysis of the two-axis X-Y table driven by PMLSM may be expressed as follows. From (11) and (13), the mechanical dynamics can be simplified as follows:

$$\ddot{d}(t) = -\frac{D}{M}\cdot\frac{2}{P}\dot{d}(t) + \frac{2}{P}\cdot\frac{K_f}{M}\cdot i_{qs}^{r*}(t) - \frac{2}{P}\cdot\frac{1}{M}(F_L + F_f(v)) \tag{15}$$

$$\ddot{d}(t) = A_m\dot{d}(t) + B_m\cdot U(t) + D_m(F_L + F_f(v)) \tag{16}$$

where $A_m = -(D/M)\cdot(P/2)$, $B_m = K_f/(M)\cdot(P/2)$, $D_m = -(P/2)\cdot(1/M)$ $U(t) = i_{qs}^{r*}(t)$ is the control effort, $\ddot{d}(t)$ is the acceleration of the mover, $\dot{d}(t)$ is the linear velocity and $d(t)$ is the position of the mover.

Now, assume that the parameters of the motion control system are well known and the external force disturbance and the frictional force are absent, rewriting (16) can represent the model of the PMLSM servo drive system.

$$\ddot{d}(t) = A_m\dot{d}(t) + B_m.U(t) \tag{17}$$

By considering the dynamics in (16) with parameter variations, disturbance and unpredictable uncertainties, then the motion equation of the system is modified to:

$$\begin{aligned}\ddot{d}(t) = {} & (A_n + \Delta A_m)\dot{d}(t) + (B_n + \Delta B_m).U(t) \\ & + (D_n + \Delta D_m)(F_L + F_f(v))\end{aligned} \tag{18}$$

$$\ddot{d}(t) = A_n\dot{d}(t) + B_n.U(t) + \Gamma(t) \tag{19}$$

where A_n, B_n and D_n are the nominal parameters of A_m, B_m and D_m respectively. ΔA_m, ΔB_m, and ΔD_m are the uncertainties due to mechanical parameters M and D, and $\Gamma(t)$ is the lumped parameter uncertainty and is defined as:

$$\Gamma(t) = \Delta A_m\dot{d}(t) + \Delta B_m.U(t) + \Lambda \tag{20}$$

The lumped parameter uncertainty is assumed to be bounded, that is,

$$|\Gamma(t)| \le \delta \tag{21}$$

where $\Lambda = (D_n + \Delta D_m)(F_L + F_f(v))$ and δ is a constant.

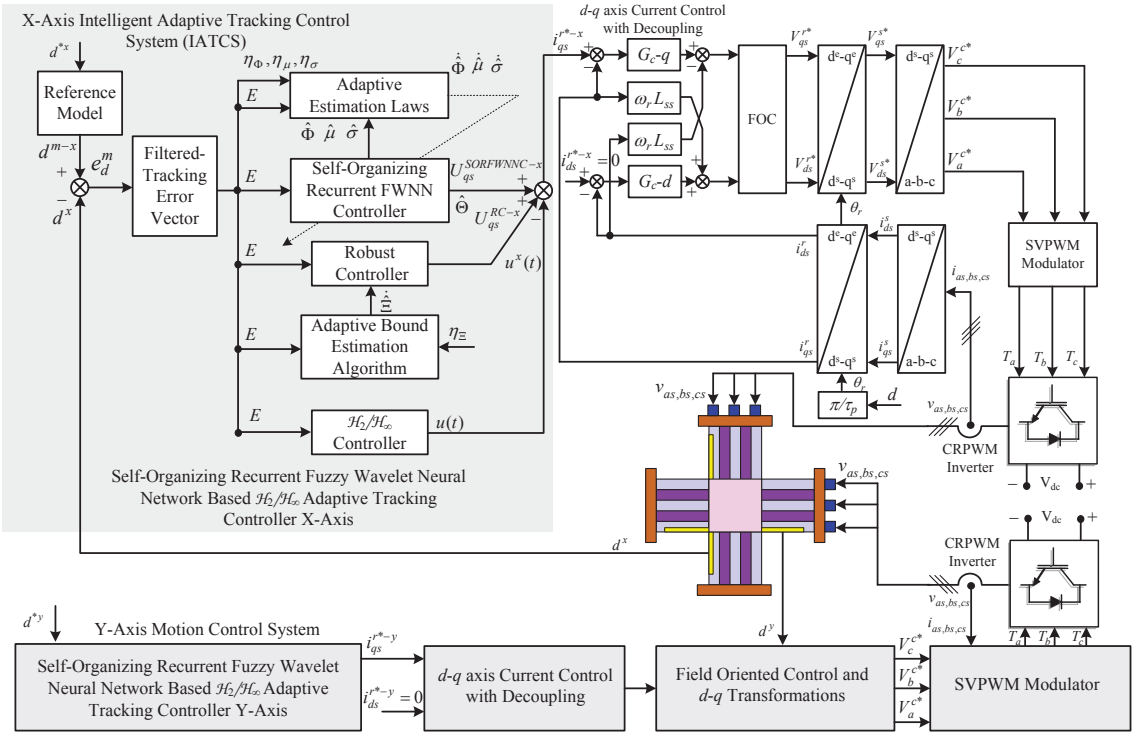

Fig. 1. Structure of the proposed IATCS with SORFWNN based mixed $\mathcal{H}_2/\mathcal{H}_\infty$ performance for two-axis motion control system

C. Problem Formulation with Mixed $\mathcal{H}_2/\mathcal{H}_\infty$ Performance

The configuration of the proposed control system is shown in Fig. 1. In this paper, the two-axis system parameter uncertainties, external disturbances, cross-coupled interference and frictional force will be considered simultaneously. Therefore, the two-axis motion control system is a nonlinear time-varying system in practical applications. The proposed design procedure is divided into three steps. First, a SORFWNN system is introduced in the next section to learn these unknown or uncertain dynamics, $\hat{\Theta}$, by adaptive algorithms. Second, a robust controller is utilized to deal with the uncertainties, including the approximation error, optimal parameter vectors and higher order terms in Taylor series. Third, the effects on the tracking error, $e_d^m(t)$, due to the unknown nonlinear dynamic function must be attenuated below a desired attenuation level ρ^2, which is, the mixed $\mathcal{H}_2/\mathcal{H}_\infty$ tracking performance is achieved. The online adaptive control laws are derived based on Lyapunov theorem and the mixed $\mathcal{H}_2/\mathcal{H}_\infty$ tracking performance so that the stability of the proposed IATCS can be guaranteed. The control law is assumed to take the form:

$$\begin{aligned} U_{IATCS}^*(t) &= B_n^{-1}[U_A + u_H] \\ &= B_n^{-1}[(U_{SORFWNNC} + U_{RC}) + u_H] \end{aligned} \tag{22}$$

where $U_A = (U_{SORFWNNC} + U_{RC})$ is the intelligent adaptive controller, $U_{SORFWNNC}$ is SORFWNNC, U_{RC} is the robust controller and u_H is the mixed $\mathcal{H}_2/\mathcal{H}_\infty$ adaptive controller.

Mixed $\mathcal{H}_2/\mathcal{H}_\infty$ adaptive control problem, for two-axis system based on the SORFWNN, under consideration is stated as follows. Consider the nonlinear tracking error dynamic in (76), (90). Given a desired disturbance attenuation level ρ^2 and weighting matrices $Q_2(t)$, $Q_\infty(t)$, $R_2(t)$ and $R_\infty(t)$, the intelligent mixed $\mathcal{H}_2/\mathcal{H}_\infty$ adaptive tracking control problem for the two-axis motion control system is said to be solved if there exist an u_H control law and an adaptive controller U_A such that the following $\mathcal{H}_2$ optimal tracking performance [34], [35]

$$\min_{u_H \in L_2[0,T]} \begin{bmatrix} E^T(t)Q_2(t)E(t)\tilde{\Phi}^T(t)\tilde{\Phi}(t) \\ + \int_0^T (E^T(t)Q_2(t)E(t) + u_H^T(t)R_2(t)u_H(t))dt \end{bmatrix} \tag{23}$$

can be achieved under the following $\mathcal{H}_\infty$ disturbance attenuation constraints [38]

$$\begin{aligned} &E^T(t)Q_\infty(t)E(t) + \tilde{\Phi}^T(t)\tilde{\Phi}(t) \\ &\quad + \int_0^T (E^T(t)Q_\infty(t)E(t) + u_H^T(t)R_\infty(t)u_H(t))dt \\ &\le E^T(0)P_\infty(0)E(0) + \frac{1}{\eta_\Phi}\tilde{\Phi}^T(0)\tilde{\Phi}(0) + \frac{1}{\eta_\mu}\tilde{\mu}^T(0)\tilde{\mu}(0) \\ &\quad + \frac{1}{\eta_\sigma}\tilde{\sigma}^T(0)\tilde{\sigma}(0) + \frac{1}{\eta_b}\tilde{b}^T(0)\tilde{b}(0) \\ &\quad + \frac{1}{\eta_c}\tilde{c}^T(0)\tilde{c}(0) + \rho^2 \int_0^T \tilde{\Lambda}^T(t)\tilde{\Lambda}(t)dt \end{aligned} \tag{24}$$

for all $\forall T \in [0,\infty]$ and for some symmetric positive matrices $Q_2(t)$, $Q_\infty(t)$, $R_2(t)$, $R_\infty(t)$, $P_2(t)$ and $P_\infty(t)$.

In this paper, we assume that $\tilde{\Theta}(t)$ is uncertain and bounded. However, the effect of $\tilde{\Theta}(t)$ will deteriorate the control performance and even lead to instability of the

nonlinear two-axis motion control system. Therefore, how to eliminate the effect of $\tilde{\Theta}(t)$ to guarantee control performance is an important design. Let us consider the following $\mathcal{H}_\infty$ control performance [32]-[35], [38]

$$\begin{aligned} J_\infty(u_H,\Lambda) &= E^T(t)Q_\infty(t)E(t)+\frac{1}{\eta_\Phi}\tilde{\Phi}^T(t)\tilde{\Phi}(t)+\frac{1}{\eta_\mu}\tilde{\mu}^T(t)\tilde{\mu}(t) \\ &+\frac{1}{\eta_\sigma}\tilde{\sigma}^T(t)\tilde{\sigma}(t)+\frac{1}{\eta_b}\tilde{b}^T(t)\tilde{b}(t)+\frac{1}{\eta_c}\tilde{c}^T(t)\tilde{c}(t) \\ &+\int_0^T\{E^T(t)Q_\infty(t)E(t)+u_H^T(t)R_\infty(t)u_H(t) \\ &-\rho^2\tilde{\Lambda}^T(t)\tilde{\Lambda}(t)\}dt \end{aligned} \tag{25}$$

where $E(t)$ is the tracking error dynamics, T is the terminal time of control, η_Φ, η_μ, η_σ η_b, η_c and η_γ are strictly positive learning rates and ρ is a prescribed attenuation constant. $Q_\infty = Q_\infty^T > 0$ is specified according to the design purpose and $P_\infty = P_\infty^T > 0$ is a weighting positive definite matrix. However, the $\mathcal{H}_\infty$ robustness performance in (25), which has been considered to eliminate the effect of $\hat{\Theta}(t)$ in the nonlinear two-axis system of (19), is not enough by itself to achieve a desired control performance. In general, the $\mathcal{H}_2$ optimal control is more appealing for control engineers to achieve a desired control performance via a proper choice of weighting matrices. The following control performance [32]-[35], [38]

$$\begin{aligned} J_2(u_H,\Lambda) &= E^T(t)Q_2(t)E(t)+\frac{1}{\eta_\Phi}\tilde{\Phi}^T(t)\tilde{\Phi}(t)+\frac{1}{\eta_\mu}\tilde{\mu}^T(t)\tilde{\mu}(t) \\ &+\frac{1}{\eta_\sigma}\tilde{\sigma}^T(t)\tilde{\sigma}(t)+\frac{1}{\eta_b}\tilde{b}^T(t)\tilde{b}(t)+\frac{1}{\eta_c}\tilde{c}^T(t)\tilde{c}(t) \\ &+\int_0^T[E^T(t)Q_2(t)E(t)+u_H^T(t)R_2(t)u_H(t)]dt \end{aligned} \tag{26}$$

must be minimized without considering $\tilde{\Theta}(t)$ and the weighting matrices $Q_2 = Q_2^T > 0$ and $R_2 = R_2^T > 0$ are specified before hand according to the design purpose. Then, the mixed $\mathcal{H}_2/\mathcal{H}_\infty$ adaptive control problem for the two-axis motion control system is equivalent to finding an optimal control law u_H^*, which is related to the mixed $\mathcal{H}_2/\mathcal{H}_\infty$ control performance and the intelligent adaptive controller U_A that include the worst case uncertainties $\Theta(t)$ such that

$$\begin{cases} J_\infty(u_H^*,\Lambda^*) \geq J_\infty(u_H^*,\Lambda), \forall \Lambda \in L_2[0,T] \\ J_2(u_H^*,\Lambda^*) \leq J_2(u_H,\Lambda^*), \forall u_H \in L_2[0,T] \end{cases} \tag{27}$$

III. Self-Organizing Recurrent Fuzzy Wavelet Neural Network (SORFWNN) Model

A. Description of the SORFWNN

The proposed SORFWNN integrates wavelet functions with TSK fuzzy model. The kernel of the fuzzy system is the fuzzy knowledge base that consists of the input–output data points of the system interpreted into linguistic fuzzy rules. The consequent parts of TSK-type fuzzy IF–THEN rules are represented by either a constant or a function. In most fuzzy and neuro-fuzzy models, the function is a linear combination of the input variables plus a constant term. TSK-type systems cannot, in general, model complex processes with desired accuracy using a certain number of rules. These systems do not have localizability, instead model the global features of the process, and their convergence is generally slow. The consequent part of this TSK-type fuzzy networks do not provide full mapping capabilities, and, in the case of modeling of complex nonlinear processes, may require a high number of rules in order to achieve the desired accuracy. Increasing the number of the rules leads to an increase in the number of neurons in the hidden layer of the network. In this paper, the use of wavelet (rather than linear) functions are proposed to improve the computational power of the neuro-fuzzy system [10]-[15]. The rules have the following form:

IF x_1 is A_1^j and x_2 is A_2^j and ... and x_n is A_n^j
THEN

$$\Psi_l(x_i) = \sum_{i=1}^{n}\omega_{il}\left(1-\left(\frac{x_i-b_{il}}{c_{il}}\right)^2\right)\exp\left(-\frac{1}{2}\left(\frac{x_i-b_{il}}{c_{il}}\right)^2\right) \tag{28}$$

where $x_i = \{x_1, x_2, \ldots, x_n\}$ are the input variables, A_n^j is the jth Gaussian type membership function for the jth input and $\Psi_l(x_i)$, which is a function of inputs, is the lth output of the fuzzy rule, b_{il} and c_{il} are the translation and the dilation parameters of the wavelet function between the ith (i=1,…,n), ω_{il} are the weights between the hidden and output layers of the WNN and the lth output (l=1,…,n). The Mexican Hat wavelet function $\psi(x) = (1-x^2)\exp(-x^2/2)$ is used as the wavelet transform in this paper. The translated and dilated version of the Mexican Hat wavelet function is used, which is given by the following equation:

$$\psi\left(\frac{x-b_j}{c_j}\right) = \left(1-\left(\frac{x-b_j}{c_j}\right)^2\right)\exp\left(-\frac{1}{2}\left(\frac{x-b_j}{c_j}\right)^2\right) \tag{29}$$

B. Structure of the SORFWNN

This subsection presents the structure of the SORFWNN model illustrated in Fig. 3. The goal of integrating this model is to improve the accuracy of function approximation.

The jth rule of the SORFWNN is presented as follows:

R_j :
IF x_1 is A_1^j and x_2 is A_2^j ... and x_n is A_n^j
THEN $h_j(N+1)$ is γ_j and $y_o^{(6)}(N+1)$ is $\sum_{j=1}^{M} y_j^{(4)}.y_l.\varpi_j$ (30)

where R_j is the jth rule; h_j is the internal variable, A_i^j is a fuzzy set, $h_j(N+1)$ is the output of the recurrent layer; $y_j^{(4)}$

is the output of layer 4; γ_j, W_{jk} and ϖ_j are the consequent part parameters for the outputs h_j, $y_j^{(4)}$ and y_l, respectively; $y_o^{(6)}$ is the output of the SORFWNN.

The architecture of the SORFWNN is a six-layer recurrent FWNN embedded with dynamic feedback connections as shown in Fig. 2. To give a clear understanding of the mathematical function of each node, we describe the basic functions and signal propagation of each layer as follows.

Layer 1: input layer: Each node in this layer is an input node, which corresponds to one input variable. These nodes only pass the input signal to the next layer and the input variables of the SORFWNN are the same. In this layer, the node input and the node output are represented as

$$net_i^{(1)}(N) = x_i^{(1)} \tag{31}$$

$$y_i^{(1)}(N) = f_i^{(1)}(net_i^{(1)}(N)) = net_i^{(1)}(N) \quad i = 1,2 \tag{32}$$

$$x_1^{(1)} = e_d^m(t) \tag{33}$$

$$x_2^{(1)} = \dot{e}_d^m(t) \tag{34}$$

where $x_i^{(1)}$ represents the ith input to the node of layer 1, N denotes the number of iterations. The input variables are $x_1^{(1)} = e_d^m = (d^m - d\ )$, the tracking position error between the desired position command $d^m(t)$, and the rotor position $d(t)$ and $x_2^{(1)} = \dot{e}_d^m = (\dot{d}^m - \dot{d})$, position error change.

Layer 2: membership layer: In this layer, each node of the SORFWNN acts as a linguistic label of one of the input variables in layer 1, i.e., the membership value specified the degree to which an input value belongs to a fuzzy set is determined in this layer. The Gaussian function is adopted as the membership function: For the jth node the input and output of the membership node can be described as follows:

$$\lambda_{A_i^j}(x_i) = \exp\left[-\frac{1}{2}\frac{(x_i - \mu_{ij})^2}{\sigma_{ij}^2}\right], \quad i = 1,\ldots,n, \quad j = 1,\ldots,m \tag{35}$$

$$net_j^{(2)}(N) = \left[-\frac{1}{2}\frac{(x_i - \mu_{ij})^2}{\sigma_{ij}^2}\right] \tag{36}$$

$$y_{ij}^{(2)}(N) = A_i^j(x_i^{(2)}) = f_j^{(2)}(net_j^{(2)}(N)) = \exp(net_j^{(2)}(N)) = \exp\left[-\frac{1}{2}\frac{(x_i - \mu_{ij})^2}{\sigma_{ij}^2}\right] \tag{37}$$

where n is the number of external input signals, m is the number of fuzzy rules, μ_{ij} and σ_{ij} are the mean and standard deviation of the Gaussian function of the SORFWNN in the jth term of the ith input linguistic variable x_i^2 to the node of layer 2, respectively, $\lambda_{A_i^j}(x_i)$ is the membership function of the ith input variable for the jth term.

Layer 3: rule layer: Each node in this layer represents one fuzzy logic rule and performs precondition matching of a rule. Thus, the neuron in this layer is denoted by Π, which multiplies the incoming signals from layer 2 and outputs the product result, i.e., the firing strength of a rule. For the jth rule node:

$$net_j^{(3)}(N) = \prod_i^n \varpi_{jk}^{(3)} y_{ij}^{(2)}(N) \tag{38}$$

$$y_j^{(3)}(N) = f_j^{(3)}(net_j^{(3)}(N)) = net_j^{(3)}(N) = \prod_{i=1}^n \varpi_{jk}^{(3)} y_{ij}^{(2)}(N) = \prod_{i=1}^n \varpi_{jk}^{(3)} \exp\left[-\frac{1}{2}\frac{(x_i - \mu_{ij})^2}{\sigma_{ij}^2}\right] \tag{39}$$

where $x_j^{(3)}$ represents the jth input to the node of layer 3; $\varpi_{jk}^{(3)}$ are the weights between the membership layer and the rule layer and are set to be equal to unity to simplify the implementation for the real-time control; and n is the number of rules.

Layer 4: recurrent layer: This layer is a recurrent layer. For the internal variable h_j in the recurrent layer, the following sigmoid membership function is used:

$$F_j = \frac{1}{1 + \exp(-\gamma_j h_j)}, \qquad j=1, 2,\ldots,m \tag{40}$$

$$h_j(N+1) = y_j^{(3)}(N) + F_j = \prod_{i=1}^n \varpi_{jk}^{(3)} \exp\left[-\frac{1}{2}\frac{(x_i - \mu_{ij})^2}{\sigma_{ij}^2}\right] + \frac{1}{1 + \exp(-\gamma_j h_j)} \tag{41}$$

where h_j is the recurrent unit acting as the memory element and γ_j is the recurrent weight.

Layer 5: wavelet layer: The neuron in this layer multiplies the incoming signals, which are h_j from the output of layer 4 (recurrent layer) and the output signal from the wavelet functions y_l. The output of the lth wavelet is calculated as

$$y_l(x_i) = \Psi_l(x_i) = \sum_{i=1}^n \omega_{il} \left|c_j\right|^{-\frac{1}{2}} \cdot \left(1 - \left(\frac{x_i - b_{il}}{c_{il}}\right)^2\right) \exp\left(-\frac{1}{2}\left(\frac{x_i - b_{il}}{c_{il}}\right)^2\right) \tag{42}$$

Furthermore, the process of this layer is described as follows:

$$net_j^{(5)}(N) = \prod_i^n y_l(x_i).y_j^{(4)}(N) \tag{43}$$

$$y_j^{(5)}(N) = f_j^{(5)}(net_j^{(5)}(N)) = net_j^{(5)}(N) = \left(\prod_{i=1}^n \varpi_{jk}^{(3)} \exp\left[-\frac{1}{2}\frac{(x_i - \mu_{ij})^2}{\sigma_{ij}^2}\right] + \frac{1}{1 + \exp(-\gamma_j h_j)}\right). \sum_{i=1}^n \omega_{il} \left|c_j\right|^{-\frac{1}{2}} \left(1 - \left(\frac{x_i - b_{il}}{c_{il}}\right)^2\right) \exp\left(-\frac{1}{2}\left(\frac{x_i - b_{il}}{c_{il}}\right)^2\right) \tag{44}$$

Layer 6: output layer: In this layer, the final output of the SORFWNN, $y_o^{(6)}$, is calculated and the output node together with related links acts as a defuzzifier. The mathematical function is given by:

$$net_o^{(6)}(N) = \sum_{j=1}^{M} y_j^{(4)}.y_l.\varpi_j \tag{45}$$

$$\begin{aligned} y_o^{(6)}(N) &= f_o^{(6)}(net_o^{(6)}(N)) = net_o^{(6)}(N) \\ &= \sum_{j=1}^{M} y_j^{(4)}.y_l.\varpi_j \\ &= U_{qs}^{SORFWNN} = \hat{\Theta}(x) \end{aligned} \tag{46}$$

where the link weight ϖ_j is the output strength and $y_o^{(6)}$ is the output of the SORFWNNC and also is the estimated nonlinear function $\hat{\Theta}$. Moreover, $y_o^{(6)} = U_{qs}^{SORFWNN}(t) = \hat{\Theta}$ for the uncertainty estimation of the X-Y table; M is the number of rules and $U_{qs}^{SORFWNNC}$ is the control effort of the single-axis mechanism of the *x-y* table motion control system. Define the vectors μ, σ, γ, $\varpi_j = \varpi$, $\omega_l = \alpha$, $b_l = \beta$ and $c_l = \zeta$ collecting all parameters of the hidden layer in the SORFWNN as:

$$\begin{cases} \varpi = [\varpi_{1o}, \varpi_{2o}, \ldots, \varpi_{Mo}], & \alpha = [\alpha_{1j}, \alpha_{2j}, \ldots, \alpha_{lj}] \\ \beta = [\beta_{1j}, \beta_{2j}, \ldots, \beta_{lj}], & \zeta = [\zeta_{1j}, \zeta_{2j}, \ldots, \zeta_{lj}] \\ \gamma = [\gamma_{1j}, \gamma_{2j}, \ldots, \gamma_{ij}], & \mu = [\mu_{1j}, \mu_{2j}, \ldots, \mu_{ij}] \\ \sigma = [1/\sigma_{1j}^2, 1/\sigma_{2j}^2, \ldots, 1/\sigma_{ij}^2] \end{cases} \tag{47}$$

The output of the SORWFNNC can be rewritten as

$$\begin{aligned} U_{qs}^{SORFWNNC} &= \Theta_{SORFWNNC}(E, \Phi, \sigma, \mu, b, c) \\ &= \Phi^T \Omega(E, \sigma, \mu, b, c) \end{aligned} \tag{48}$$

where the tracking error vector E is the input of the SORFWNN, $\Phi = [\Phi_1, \Phi_2, \ldots\ldots, \Phi_M]^T$ is the adjustable weights vector (γ, ϖ, ω), Ω is the output vector $(\sigma, \mu, \beta, \zeta, \Psi_l, h_j)$ and $E = [e_d^m \quad \dot{e}_d^m]^T$ is the tracking error input vector to the SORFWNN controller. It was proved that there exists an SORFWNN as shown in (48) such that it can uniformly approximate a nonlinear, even time-varying function [24].

C. On-Line Learning Algorithms of the SORFWNN

1) Structure Learning Algorithm: The structure learning algorithm is responsible for on-line rule generation. The first step in structure learning is to determine when to generate a new rule. The way the input space is partitioned determines the number of rules extracted from the training data, as well as the number of fuzzy sets in the universe of discourse for each input variable because one cluster in the input space corresponds to one fuzzy rule, in which μ_{ij} represents the mean and σ_{ij} represents the standard deviation of that cluster, respectively. For each incoming pattern x_i, the rule firing strength can be regarded as the degree to which the incoming pattern belongs to the corresponding cluster. For computational efficiency, the degree measure can be calculated using the firing strength from (38) as

$$D_j = y_j^{(3)}, \quad j = 1, \ldots, M(t) \tag{49}$$

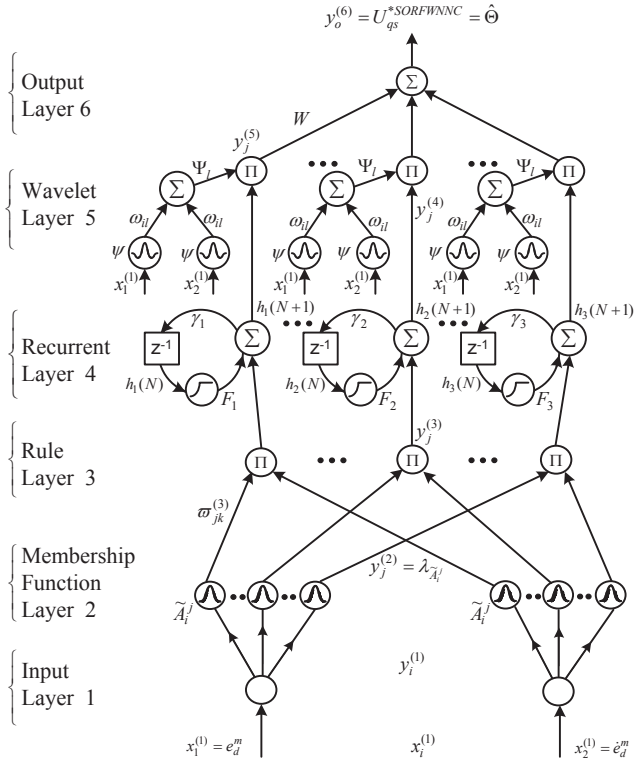

Fig. 2. Structure of self-organizing recurrent fuzzy wavelet neural network (SORFWNN) model

where $M(t)$ denotes the number of existing rules at time t and $D_j \in [0,1]$. According to the degree measure, the criterion for the generation of a new fuzzy rule for a new incoming data is described as follows. Find the maximum degree $D_{\max}$

$$D_{\max} = \max_{1 \le j \le M(t)} D_j \tag{50}$$

If $D_{\max} \le D$, then a new rule is generated, where $D \in [0,1]$ is a prescribed threshold that decays during the learning process, thus limiting the size of the SORFWNN. Once a new rule has been generated, the next step is to assign the initial mean and standard deviation to the new membership function and the corresponding link weight for the consequent part. Since the goal is to minimize an objective function, the mean, standard deviation and weights are all adjustable later in the parameter learning phase. Hence, the mean, standard deviation, translation, dilation and weights for the new rule are set as follows:

$$\mu_{ij}^{M(t+1)} = x_i(t) \tag{51}$$

$$\sigma_{ij}^{M(t+1)} = \sigma_{init} \tag{52}$$

$$\alpha_{ij}^{M(t+1)} = r \tag{53}$$

$$\beta_{ij}^{M(t+1)} = r \tag{54}$$

$$\gamma_{ij}^{M(t+1)} = r \tag{55}$$

$$\zeta_{ij}^{M(t+1)} = r \tag{56}$$

$$\varpi_{ij}^{M(t+1)} = r \tag{57}$$

where x_i is the new input, $r \in [-1,+1]$ is a random variable and σ_{init} is a prespecified constant.

2) Parameter Learning Algorithm: After the network structure has been adjusted according to the current pattern, the network then begins parameter learning to adjust the parameters of the membership functions optimally with the same training pattern. The central part of the parameter learning algorithm for the SORFWNN concerns how to recursively obtain a gradient vector in which each element in the learning algorithm is defined as the derivative of an energy function with respect to a parameter of the network. This is done by means of the chain rule and the method is generally referred to as the backpropagation learning rule, because the gradient vector is calculated in the direction opposite to the flow of the output of each node. The parameter learning is based on supervised learning algorithm to adjust the connected weights in the consequent part, the feedback weights and the parameters of the membership functions using the backpropagation algorithm to minimize a given energy function. To describe the on-line parameter learning algorithm, the energy function E_d is defined as

$$E_d = \frac{1}{2}(d^m - d\ )^2 = \frac{1}{2}(e_d^m)^2 \tag{58}$$

where $d^m(t)$ is the desired motion, $d(t)$ is the actual motion of the mover of the PMLSM and e_d^m is the error signal between the desired motion and the actual motion.

Then, the update laws for the parameters in the SORFWNN are described as follows:

The update law of ϖ_j is

$$\Delta\varpi_j = -\eta_\varpi \frac{\partial E_d}{\partial \varpi_j} = \left[-\eta_\varpi \frac{\partial E_d}{\partial y_o^{(6)}} \frac{\partial y_o^{(6)}}{\partial \varpi_j} \right] = \eta_\varpi \delta_o^{(6)} y_j^{(5)} \tag{59}$$

The weights of the output layer (layer 6) are updated according to the following equation.

$$\varpi_j(N+1) = \varpi_j(N) + \Delta\varpi_j(N) \tag{60}$$

The update law of ω_l is:

$$\begin{aligned} \Delta\omega_l &= -\eta_\omega \frac{\partial E_d}{\partial \omega_l} = \left[-\eta_\omega \frac{\partial E_d}{\partial y_o^{(6)}} \frac{\partial y_o^{(6)}}{\partial y_j^{(5)}} \frac{\partial y_j^{(5)}}{\partial y_l} \frac{\partial y_l}{\partial \omega_l} \right] \\ &= \eta_\omega \delta_j^{(5)} y_j^{(4)} \Psi_l \end{aligned} \tag{61}$$

The update law of b_l is:

$$\begin{aligned} \Delta b_l &= -\eta_b \frac{\partial E_d}{\partial b_l} = \left[-\eta_b \frac{\partial E_d}{\partial y_o^{(6)}} \frac{\partial y_o^{(6)}}{\partial y_j^{(5)}} \frac{\partial y_j^{(5)}}{\partial y_l} \frac{\partial y_l}{\partial \Psi_l} \frac{\partial \Psi_l}{\partial \vartheta_l} \frac{\partial \vartheta_l}{\partial b_l} \right] \\ &= \eta_b \delta_l \ \frac{1}{c_{il}} \left(\frac{x_i - b_{il}}{c_{il}} \right) \left(3 - \left(\frac{x_i - b_{il}}{c_{il}} \right)^2 \right) \exp\left(-\frac{1}{2} \left(\frac{x_i - b_{il}}{c_{il}} \right)^2 \right) \\ &= \eta_b \delta_l \ \frac{1}{c_{il}} (3\vartheta_{il} - \vartheta_{il}^2) \exp(-\vartheta_{il}^2 / 2) \end{aligned} \tag{62}$$

The update law of c_l is:

$$\begin{aligned} \Delta c_l &= -\eta_c \frac{\partial E_d}{\partial c_l} = \left[-\eta_b \frac{\partial E_d}{\partial y_o^{(6)}} \frac{\partial y_o^{(6)}}{\partial y_j^{(5)}} \frac{\partial y_j^{(5)}}{\partial y_l} \frac{\partial y_l}{\partial \Psi_l} \frac{\partial \Psi_l}{\partial \vartheta_l} \frac{\partial \vartheta_l}{\partial c_l} \right] \\ &= \eta_c \delta_l \left(\frac{x_i - b_{il}}{c_{il}} \right)^2 \left(3 - \left(\frac{x_i - b_{il}}{c_{il}} \right)^2 \right) \exp\left(-\frac{1}{2} \left(\frac{x_i - b_{il}}{c_{il}} \right)^2 \right) \\ &= \eta_b \delta_l \ (3\vartheta_{il}^2 - \vartheta_{il}^4) \exp(-\vartheta_{il}^2 / 2) \end{aligned} \tag{63}$$

The weights of the wavelet layer (layer 5) are updated according to the following equations.

$$\omega_l(N+1) = \omega_l(N) + \Delta\omega_l(N) \tag{64}$$

$$b_l(N+1) = b_l(N) + \Delta b_l(N) \tag{65}$$

$$c_l(N+1) = c_l(N) + \Delta c_l(N) \tag{66}$$

The update law of γ_j is:

$$\begin{aligned} \Delta\gamma_j &= -\eta_\gamma \frac{\partial E_d}{\partial \gamma_j} = \left[-\eta_\gamma \frac{\partial E_d}{\partial y_j^{(4)}} \frac{\partial y_j^{(4)}}{\partial F_j} \frac{\partial F_j}{\partial h_j} \frac{\partial h_j}{\partial \gamma_j} \right] \\ &= \eta_\gamma \delta_j^{(4)} F_j\ (1 - F_j\ ) y_j^{(4)} (N-1) \prod_{i=1}^{n} y_j^{(3)}(N) \end{aligned} \tag{67}$$

The weights of the recurrent layer (layer 4) are updated according to the following equation.

$$\gamma_j(N+1) = \gamma_j(N) + \Delta\gamma_j(N) \tag{68}$$

The update laws of means are:

$$\begin{aligned} \Delta\mu_{ij} &= -\eta_\mu \frac{\partial E_d}{\partial \mu_{ij}} = \left[-\eta_\mu \frac{\partial E_d}{\partial \lambda_{A_i^j}} \frac{\partial \lambda_{A_i^j}}{\partial \mu_{ij}} \right] \\ &= \eta_\mu \delta_j^2 \varpi_{jk}^3 \frac{2(x_i^2 - \mu_{ij})}{(\sigma_{ij})^2} \end{aligned} \tag{69}$$

Moreover, the update law of the standard deviation is:

$$\begin{aligned} \Delta\sigma_{ij} &= -\eta_\sigma \frac{\partial E_d}{\partial \sigma_{ij}} = \left[-\eta_\sigma \frac{\partial E_d}{\partial \lambda_{A_i^j}} \frac{\partial \lambda_{A_i^j}}{\partial \sigma_{ij}} \right] \\ &= \eta_\sigma \delta_j^2 \varpi_{jk}^3 \frac{2(x_i^2 - \sigma_{ij})^2}{(\sigma_{ij})^3} \end{aligned} \tag{70}$$

The weights of the membership layer (layer 2) are updated according to the following equations.

$$\mu_{ij}(N+1) = \mu_{ij}(N) + \Delta\mu_{ij}(N) \tag{71}$$

$$\sigma_{ij}(N+1) = \sigma_{ij}(N) + \Delta\sigma_{ij}(N) \tag{72}$$

where η_ϖ, η_γ, η_ω, η_b, η_c, η_μ and η_σ are the learning-rate parameters of the connected weights and the link weights of the FWNN, feedback weights, and translation and dilation of the membership functions of the SORFWNN, respectively and N denotes the iteration number of the jth link.

IV. Design of the Intelligent Adaptive Tracking Control System (IATCS)

The control problem is to find a control law so that the actual motion $d(t)$ can track the desired command motion

$d^m(t)$. Since the parameter uncertainties of the two-axis motion control system are difficult to measure, the SORFWNN controller is proposed to approximate the nonlinear function Θ, which contains the effects of parameter variations, external disturbances, the cross-coupled interference and the frictional force while the robust controller is used to compensate the approximation error of the SORFWNN controller, optimal parameter vectors and higher order terms in Taylor series. The effects on the tracking error, $e_d^m(t)$, due to the UNDF Θ must be attenuated below a desired attenuation level ρ^2, which is, the mixed $\mathcal{H}_2/\mathcal{H}_\infty$ tracking performance is achieved.

A. Ideal Control of the Two-Axis X-Y Table

The control problem is to find a control law so that the state $d(t)$ can track the desired motion command $d^m(t)$. To achieve this control objective, a tracking error vector is defined as

$$E = [d^m - d \quad \dot{d}^m - \dot{d}]^T = [e_d^m \quad \dot{e}_d^m]^T \tag{73}$$

where $d^m(t)$ and $\dot{d}^m(t)$ are the desired motion and velocity of the two-axis motion control system; $e_d^m(t)$ and $\dot{e}_d^m(t)$ denote the motion and velocity errors.

The ideal controller can be designed as follows:

$$\begin{aligned} u_{IC}(t) &= B_n^{-1}[\ddot{d}^m(t) - A_n\dot{d}(t) - \Gamma(t) + k_2\dot{e}_d(t) + k_1 e_d(t)] \\ &= B_n^{-1}[\ddot{d}^m(t) - A_n\dot{d}(t) - \Gamma(t) + KE] \end{aligned} \tag{74}$$

where $K = [k_1 \quad k_2]$, in which k_1 and k_2 are positive constants. Substituting (23) into (19) yields

$$\ddot{e}_d^m(t) + k_2\dot{e}_d^m(t) + k_1 e_d^m(t) = 0 \tag{75}$$

In (81) if the control gains k_2 and k_1 are chosen to correspond to the coefficients of Hurwitz polynomial, it implies that tracking error will converge to zero when time tends to infinity. However, in practical applications, the lumped uncertainty can not be precisely known. Therefore, the ideal controller (IC) in (74) is unobtainable and can not guarantee the performance specified by (75). Moreover, to ensure the stability of the two-axis motion control system despite the existence of the uncertain dynamics, external load disturbance, cross-coupled interference and frictional force, an IATCS is proposed to mimic the IC and to estimate the value of lumped parameter uncertainty of the two-axis motion control system online in the following section.

B. Design of the SORFWNN-Based Mixed $\mathcal{H}_2/\mathcal{H}_\infty$ Adaptive Tracking Control System

The control objective is to ensure that the X-Y table system tracks desired trajectories despite of uncertainties exist in the dynamic model. To quantify the tracking objective, a filtered-tracking error function denoted by $E(t)$ is defined as $E(t) = \dot{e}_d(t) + k_1 e_d(t) + k_2\int e_d(\tau)d\tau$,. From (19), (20) and the differentiation of tracking error function $E(t)$, the tracking error dynamics can be expressed as

$$\begin{aligned} B_n^{-1}\dot{E}(t) &= B_n^{-1}A_n E(t) - u_{IC}(t) + \Theta - \Lambda \\ &= B_n^{-1}A_n E(t) + (U_{SORFWNNC}(t) + U_{RC}(t) - \Lambda + u_H(t)) \\ &= B_n^{-1}A_n E(t) + (\Theta + U_{RC}(t) - \Lambda - u(t)) \end{aligned} \tag{76}$$

$$\Theta = B_n^{-1}\begin{pmatrix} [\ddot{d}^m(t) + k_1\dot{e}_d(t) + k_2 e_d(t)] - A_n[\dot{d}^m(t) \\ + k_1 e_d(t) + k_2\int e_d(\tau)d\tau] - \Gamma(t) + \Lambda \end{pmatrix} \tag{77}$$

$$u_{IC}(t) = \Theta - u(t) \tag{78}$$

$$u(t) = B_n^{-1}\dot{E}(t) - B_n^{-1}A_n E(t) \tag{79}$$

From (77), the nonlinear function, Θ, contains the effects of mechanical parameter variations, external disturbances, the cross-coupled interference and the frictional force. Since the parameter variations of the two-axis motion control system are difficult to measure and the exact value of the external disturbances, cross-coupled interference and frictional force are also difficult to know in advance for practical applications, the control law shown in (78) can not implemented practically and the performance specified by (75) can not guarantee. Moreover, to ensure the stability of the X-Y table system despite the existence of the uncertain dynamics, an SORFWNNC is proposed to approximate the nonlinear function, Θ. Moreover the control law is designed as

$$U_{qs}(t) = \hat{\Theta}(x) - u(t) \tag{80}$$

where the intelligent controller using SORFWNN, $\hat{\Theta}(x)$, is used to learn the nonlinear function Θ and is defined as

$$\hat{\Theta}(x) = \hat{\Theta}_{SORFWNNC} + U_{RC}(t) \tag{81}$$

The control law is assumed to take the following form:

$$U_{qs}(t) = i_{qs}^*(t) = U_{SORFWNNC}(t) + U_{RC}(t) + u_H(t) \tag{82}$$

where $\hat{\Theta}_{SORFWNNC}$ is the SORFWNN controller, $U_{RC}(t)$ is a robust controller and $u_H(t)$ is the mixed $\mathcal{H}_2/\mathcal{H}_\infty$ tracking controller or the auxiliary controller. The intelligent controller is used to learn the nonlinear equation Θ due to the uncertain two-axis motion control system dynamics, the robust control $U_{RC}(t)$ is designed to compensate for the difference between Θ and $\hat{\Theta}^{SORFWNNC}$, and $u_H(t)$ is designed based on the mixed $\mathcal{H}_2/\mathcal{H}_\infty$ tracking performance to force the X-Y table system to follow the desired trajectory and to attenuate the external disturbances.

1) Approximation of SORFWNN

The output of the SORWFNN controller can be rewritten as

$$\Theta_{SORFWNNC} = \Phi^T\Omega \tag{83}$$

According to the universal approximation property [36], [37], there exists an optimal SORFWNN controller $\Theta_{SORFWNNC}^*$ to learn the nonlinear function Θ such that

$$\Theta_{SORFWNNC}^*(E, \Phi^*, \mu^*, \sigma^*, b^*, c^*) + \varepsilon = \Phi^{*T}\Omega^* + \varepsilon \tag{84}$$

where ε is a minimum reconstructed error; and Φ^*, μ^* σ^*, b^* and c^* are the optimal parameters of Φ, μ, σ, b and c, respectively, in the SORFWNN. Rewriting (89), we obtain

$$\hat{\Theta}_{SORFWNNC}(E,\hat{\Phi},\hat{\mu},\hat{\sigma},\hat{b},\hat{c})+U_{RC}=\hat{\Phi}^T\hat{\Omega}+U_{RC} \tag{85}$$

where $\hat{\Phi}$, $\hat{\mu}$ and $\hat{\sigma}$ are the estimated values of the optimal parameters as provided by the tuning algorithms that will be introduced. Subtracting (85) from (84), the approximation error, $\tilde{\Theta}$, is defined as:

$$\begin{aligned}\tilde{\Theta}&=\Theta-\hat{\Theta}=\Phi^{*T}\Omega^*+\varepsilon-\hat{\Phi}^T\hat{\Omega}-U_{RC}\\&=\tilde{\Phi}^T\Omega^*+\hat{\Phi}^T\tilde{\Omega}+\varepsilon-U_{RC}\end{aligned} \tag{86}$$

where $\tilde{\Phi}=(\Phi^*-\hat{\Phi})$ and $\tilde{\Omega}=(\Omega^*-\hat{\Omega})$. The weights of the SORFWNN are updated online to make its output approximate the unknown nonlinear function Θ accurately. To achieve this goal, the linearization technique is used to transform the nonlinear output of SORFWNN into partially linear form so that the Lyapunov theorem extension can be applied. The expansion of $\tilde{\Omega}$ in Taylor series is obtained as:

$$\begin{aligned}\tilde{\Omega}&=\begin{bmatrix}\tilde{\Omega}_1\\\tilde{\Omega}_2\\\vdots\\\tilde{\Omega}_j\end{bmatrix}=\left.\begin{bmatrix}\frac{\partial\Omega_1}{\partial\mu}\\\frac{\partial\Omega_2}{\partial\mu}\\\vdots\\\frac{\partial\Omega_j}{\partial\mu}\end{bmatrix}^T\right|_{\mu=\hat{\mu}}\tilde{\mu}+\left.\begin{bmatrix}\frac{\partial\Omega_1}{\partial\sigma}\\\frac{\partial\Omega_2}{\partial\sigma}\\\vdots\\\frac{\partial\Omega_j}{\partial\sigma}\end{bmatrix}^T\right|_{\sigma=\hat{\sigma}}\tilde{\sigma}\\&\quad+\left.\begin{bmatrix}\frac{\partial\Omega_1}{\partial b}\\\frac{\partial\Omega_2}{\partial b}\\\vdots\\\frac{\partial\Omega_j}{\partial b}\end{bmatrix}^T\right|_{b=\hat{b}}\tilde{b}+\left.\begin{bmatrix}\frac{\partial\Omega_1}{\partial c}\\\frac{\partial\Omega_2}{\partial c}\\\vdots\\\frac{\partial\Omega_j}{\partial c}\end{bmatrix}^T\right|_{c=\hat{c}}\tilde{c}+G_\Theta\\&\equiv\Omega_\mu^T\tilde{\mu}+\Omega_\sigma^T\tilde{\sigma}+\Omega_b^T\tilde{b}+\Omega_c^T\tilde{c}+G_\Theta\end{aligned} \tag{87}$$

Rewriting (90), it can be obtained that

$$\Omega^*=\hat{\Omega}+\Omega_\mu^T\tilde{\mu}+\Omega_\sigma^T\tilde{\sigma}+\Omega_b^T\tilde{b}+\Omega_c^T\tilde{c}+G_\Theta \tag{88}$$

Substituting (91) into (89) will yield

$$\begin{aligned}\tilde{\Theta}&=\Phi^{*T}\Omega^*+\varepsilon-\hat{\Phi}^T\hat{\Omega}-U_{RC}\\&=\Phi^{*T}[\hat{\Omega}+\Omega_\mu^T\tilde{\mu}+\Omega_\sigma^T\tilde{\sigma}+\Omega_b^T\tilde{b}+\Omega_c^T\tilde{c}+G_\Theta]\\&\quad+\varepsilon-\hat{\Phi}^T\hat{\Omega}-U_{RC}\\&=\tilde{\Phi}^T\hat{\Omega}+\hat{\Phi}^T\Omega_\mu^T\tilde{\mu}+\hat{\Phi}^T\Omega_\sigma^T\tilde{\sigma}+\hat{\Phi}^T\Omega_b^T\tilde{b}\\&\quad+\hat{\Phi}^T\Omega_c^T\tilde{c}-U_{RC}+\Xi\end{aligned} \tag{89}$$

where the uncertain term

$\Xi=\tilde{\Phi}^T\Omega_\mu^T\tilde{\mu}+\tilde{\Phi}^T\Omega_\sigma^T\tilde{\sigma}+\tilde{\Phi}^T\Omega_b^T\tilde{b}+\tilde{\Phi}^T\Omega_c^T\tilde{c}+\Phi^{*T}G_\Theta+\varepsilon$.

According to (76), (79), (80), (85) and (88), the error dynamic equation can be represented as

$$\begin{aligned}B_n^{-1}\dot{E}(t)&=B_n^{-1}A_nE(t)-U_{qs}(t)+\Theta-\Lambda\\&=B_n^{-1}A_nE(t)-\hat{\Theta}+u(t)+\Theta-\Lambda\\&=B_n^{-1}A_nE(t)+u(t)+\tilde{\Theta}-\Lambda\\&=B_n^{-1}A_nE(t)+u(t)-\Lambda\\&\quad+[\tilde{\Phi}^T\hat{\Omega}+\hat{\Phi}^T\Omega_\mu^T\tilde{\mu}+\hat{\Phi}^T\Omega_\sigma^T\tilde{\sigma}+\hat{\Phi}^T\Omega_b^T\tilde{b}\\&\quad+\hat{\Phi}^T\Omega_c^T\tilde{c}-U_{RC}+\Xi]\end{aligned} \tag{90}$$

2) SORFWNN-Based Mixed $\mathcal{H}_2/\mathcal{H}_\infty$ Adaptive Control

The proposed design procedure is divided into three steps. The first is the SORFWNN controller to learn the uncertain dynamics, Θ, by adaptive algorithms that includes the uncertain dynamics, external load disturbance, the cross-coupled interference and the frictional force for the two-axis motion control system. The second is the robust controller to deal with the uncertainties, including the approximation error, optimal parameter vectors and higher order terms in Taylor series. The last is the mixed $\mathcal{H}_2/\mathcal{H}_\infty$ adaptive tracking controller to be specified such that the effects on the tracking error, $e_d^m(t)$, due to the unknown nonlinear dynamic function must be attenuated below a desired attenuation level ρ^2. For the convenience of design, we take $R_2(t)=R(t)$ and $R_\infty(t)=(3/2)R(t)$ throughout this paper. Then, we have the following results.

Theorem 1: Consider the two-axis motion control system represented by (19), the control input is chosen as (82), the intelligent control law is designed as (85), in which the adaptation laws of the SORFWNN controller are designed as (91)-(95), the robust controller is designed as (96) with the adaptive lumped uncertainty estimation algorithm given in (97) and the mixed $\mathcal{H}_2/\mathcal{H}_\infty$ adaptive tracking controller is designed as (98)-(99).

$$\dot{\hat{\Phi}}=\eta_\Phi E^TP_2B_n\hat{\Omega}^T \tag{91}$$

$$\dot{\hat{\mu}}=\eta_\mu E^TP_2B_m\hat{\Phi}^T\hat{\Omega}_\mu^T \tag{92}$$

$$\dot{\hat{\sigma}}=\eta_\sigma E^TP_2B_n\hat{\Phi}^T\hat{\Omega}_\sigma^T \tag{93}$$

$$\dot{\hat{b}}=\eta_b E^TP_2B_n\hat{\Phi}^T\hat{\Omega}_b^T \tag{94}$$

$$\dot{\hat{c}}=\eta_c E^TP_2B_n\hat{\Phi}^T\hat{\Omega}_c^T \tag{95}$$

$$U_{qs}^{RC}=\hat{\Xi}(t) \tag{96}$$

$$\dot{\hat{\Xi}}(t)=\eta_\Xi\left|E^TP_2B_n\right| \tag{97}$$

$$u_H=R^{-1}E^TP_2B_n \tag{98}$$

$$\Lambda=\rho^{-2}E^TP_\infty B_n \tag{99}$$

where η_Φ, η_μ, η_σ, η_b, η_c and η_Ξ are strictly positive learning rates, and $\hat{\Xi}(t)$ is the on-line estimated value of the uncertainty term Ξ. R^{-1} is a positive constant, P_2 and P_∞ are symmetric positive definite solution of the following coupled nonlinear differential equations

$$\dot{P}_2(t)+P_2(t)A_n+A_n^TP_2(t)+Q_2(t)$$
$$-[P_\infty(t)B_n \quad P_2(t)B_n]\times\begin{bmatrix}0 & \frac{-1}{\rho^2}\\ \frac{-1}{\rho^2} & R^{-1}(t)\end{bmatrix}\begin{bmatrix}B_n^TP_\infty(t)\\ B_n^TP_2(t)\end{bmatrix}=0 \quad (100)$$

$$\dot{P}_\infty(t)+P_\infty(t)A_n+A_n^TP_\infty(t)+Q_\infty(t)$$
$$-[P_\infty(t)B_n \quad P_2(t)B_n]\times\begin{bmatrix}\frac{-1}{\rho^2} & R^{-1}(t)\\ R^{-1}(t) & -\frac{3}{2}R^{-1}(t)\end{bmatrix}\begin{bmatrix}B_n^TP_\infty(t)\\ B_n^TP_2(t)\end{bmatrix}=0 \quad (101)$$

with the constraint $B_n^TP_2(t)=B_n^TP_\infty(t)$ and the terminal conditions $Q_2=P_2$ and $Q_\infty=P_\infty$; then the mixed $\mathcal{H}_2/\mathcal{H}_\infty$ adaptive control problem for the two-axis motion control system is solved by (82), (91)–(99).

Proof 1: By the terminal conditions $Q_\infty=P_\infty$, the constraint $B_n^TP_2(t)=B_n^TP_\infty(t)$ and the optimal control law in (98) and the update laws in (91)-(95) and (97) with the fact that $\dot{\tilde{\Phi}}(t)=\dot{\hat{\Phi}}(t),\dot{\tilde{\mu}}(t)=\dot{\hat{\mu}}(t),\dot{\tilde{\sigma}}(t)=\dot{\hat{\sigma}}(t),\dot{\tilde{b}}(t)=\dot{\hat{b}}(t),\dot{\tilde{c}}(t)=\dot{\hat{c}}(t)$, the performance index $J_\infty(u_H,\Lambda)$ in (25) can be rearranged and obtained as follows:

$$\begin{aligned}J_\infty(u_H^*,\Lambda)&=E^T(0)P_\infty(0)E(0)+\frac{1}{\eta_\Phi}\tilde{\Phi}^T(0)\tilde{\Phi}(0)+\frac{1}{\eta_\mu}\tilde{\mu}^T(0)\tilde{\mu}(0)\\&+\frac{1}{\eta_\sigma}\tilde{\sigma}^T(0)\tilde{\sigma}(0)+\frac{1}{\eta_b}\tilde{b}^T(0)\tilde{b}(0)+\frac{1}{\eta_c}\tilde{c}^T(0)\tilde{c}(0)\\&+\int_0^T\{E^T(t)[\dot{P}_\infty(t)+P_\infty(t)A_n+A_n^TP_\infty(t)+Q_\infty(t)\\&-[P_\infty(t)B_n \quad P_2(t)B_n]\\&\times\begin{bmatrix}\frac{-1}{\rho^2} & R^{-1}(t)\\ R^{-1}(t) & -\frac{3}{2}R^{-1}(t)\end{bmatrix}\begin{bmatrix}B_n^TP_\infty(t)\\ B_n^TP_2(t)\end{bmatrix}]E(t)\\&-[\rho\Lambda-\rho^{-1}B_n^TP_\infty E]^T\times[\rho\Lambda-\rho^{-1}B_n^TP_\infty E]\}dt\end{aligned} \quad (102)$$

Substituting (101) into (102) and using the control law (96), we conclude that

$$\begin{aligned}J_\infty(u_H^*,\Lambda)&=E^T(0)P_\infty(0)E(0)+\frac{1}{\eta_\Phi}\tilde{\Phi}^T(0)\tilde{\Phi}(0)+\frac{1}{\eta_\mu}\tilde{\mu}^T(0)\tilde{\mu}(0)\\&+\frac{1}{\eta_\sigma}\tilde{\sigma}^T(0)\tilde{\sigma}(0)+\frac{1}{\eta_b}\tilde{b}^T(0)\tilde{b}(0)+\frac{1}{\eta_c}\tilde{c}^T(0)\tilde{c}(0)\end{aligned} \quad (103)$$

$$J_\infty(u_H^*,\Lambda^*)\ge J_\infty(u_H^*,\Lambda),\forall\Lambda\in L_2[0,T] \quad (104)$$

Similarly, using the terminal conditions $Q_2=P_2$, By the worst case disturbance law in (99) and the update laws in (91)-(95) and (97) with the fact that $\dot{\tilde{\Phi}}(t)=\dot{\hat{\Phi}}(t),\dot{\tilde{\mu}}(t)=\dot{\hat{\mu}}(t),\dot{\tilde{\sigma}}(t)=\dot{\hat{\sigma}}(t),\dot{\tilde{b}}(t)=\dot{\hat{b}}(t),\dot{\tilde{c}}(t)=\dot{\hat{c}}(t)$, the performance index $J_2(u_H,\Lambda)$ in (26) can be rearranged as follows:

$$\begin{aligned}J_2(u_H,\Lambda^*)&=E^T(0)P_2(0)E(0)+\frac{1}{\eta_\Phi}\tilde{\Phi}^T(0)\tilde{\Phi}(0)+\frac{1}{\eta_\mu}\tilde{\mu}^T(0)\tilde{\mu}(0)\\&+\frac{1}{\eta_\sigma}\tilde{\sigma}^T(0)\tilde{\sigma}(0)+\frac{1}{\eta_b}\tilde{b}^T(0)\tilde{b}(0)+\frac{1}{\eta_c}\tilde{c}^T(0)\tilde{c}(0)\\&+\int_0^T\{E^T(t)[\dot{P}_2(t)+P_2(t)A_n+A_n^TP_2(t)+Q_2(t)\\&-[P_\infty(t)B_n \quad P_2(t)B_n]\\&\times\begin{bmatrix}0 & -\frac{1}{\rho^2}\\ -\frac{1}{\rho^2} & R^{-1}(t)\end{bmatrix}\begin{bmatrix}B_n^TP_\infty(t)\\ B_n^TP_2(t)\end{bmatrix}]E(t)\\&+[u_H+R^{-1}(t)B_n^TP_2(t)E(t)]^TR(t)[u_H\\&+R^{-1}(t)B_n^TP_2(t)E(t)]\}dt\end{aligned} \quad (105)$$

Substituting (100) into (105) and using the control law (99), we conclude that

$$\begin{aligned}J_2(u_H,\Lambda^*)&=E^T(0)P_2(0)E(0)+\frac{1}{\eta_\Phi}\tilde{\Phi}^T(0)\tilde{\Phi}(0)+\frac{1}{\eta_\mu}\tilde{\mu}^T(0)\tilde{\mu}(0)\\&+\frac{1}{\eta_\sigma}\tilde{\sigma}^T(0)\tilde{\sigma}(0)+\frac{1}{\eta_b}\tilde{b}^T(0)\tilde{b}(0)+\frac{1}{\eta_c}\tilde{c}^T(0)\tilde{c}(0)\end{aligned} \quad (106)$$

and

$$J_2(u_H^*,\Lambda^*)\ge J_2(u_H,\Lambda^*),\forall u_H\in L_2[0,T] \quad (107)$$

Theorem 2: Consider the two-axis motion control system represented by (19), if the control input is chosen as (82), the intelligent control law is designed as (84), in which the adaptation laws of the SORFWNN controller are designed as (91)-(95), the robust controller is designed as (96) with the adaptive lumped uncertainty estimation algorithm given in (97) and the mixed $\mathcal{H}_2/\mathcal{H}_\infty$ adaptive tracking controller is designed as (98)-(99) where $P_2(t)$ and P_∞(t) are symmetric positive definite solutions of the coupled non-linear differential equations in (100) and (101) with the constraint $B_n^TP_2(t)=B_n^TP_\infty(t)$, then the tracking error $E(t)$ and the estimation error $\tilde{\Theta}$ in the error dynamic system (90) are all bounded. As a result, the stability of the IATCS can be guaranteed.

Proof 2: Let us choose a Lyapunov function defined as:

$$\begin{aligned}V(E,\tilde{\Phi},\tilde{\mu},\tilde{\sigma},\tilde{b},\tilde{c},t)&=E^T(t)P_\infty(t)E(t)+\frac{1}{\eta_\Phi}\tilde{\Phi}^T(t)\tilde{\Phi}(t)+\frac{1}{\eta_\mu}\tilde{\mu}^T(t)\tilde{\mu}(t)\\&+\frac{1}{\eta_\sigma}\tilde{\sigma}^T(t)\tilde{\sigma}(t)+\frac{1}{\eta_b}\tilde{b}^T(t)\tilde{b}(t)+\frac{1}{\eta_c}\tilde{c}^T(t)\tilde{c}(t)\end{aligned} \quad (108)$$

By taking the derivative of the Lyapunov function (108) and using the optimal control law in (98), the update laws in (91)-

(95), (97), the constraint $B_n^T P_2(t) = B_n^T P_\infty(t)$ and $\dot{\widetilde{\Phi}}(t) = \widetilde{\Phi}(t), \dot{\widetilde{\mu}}(t) = \widetilde{\mu}(t), \dot{\widetilde{\sigma}}(t) = \widetilde{\sigma}(t), \dot{\widetilde{b}}(t) = \widetilde{b}(t), \dot{\widetilde{c}}(t) = \widetilde{c}(t)$, it is obtained that:

$$\begin{aligned}\dot{V}&(E,\widetilde{\Phi},\widetilde{\mu},\widetilde{\sigma},\widetilde{b},\widetilde{c},t)\\ &= E^T(t)[\dot{P}_\infty(t) + P_\infty(t)A_n + A_n^T P_\infty(t)\\ &\quad -[P_\infty(t)B_n \quad P_2(t)B_n]\\ &\quad \times\begin{bmatrix}\frac{-1}{\rho^2} & R^{-1}(t)\\ R^{-1}(t) & -\frac{3}{2}R^{-1}(t)\end{bmatrix}\begin{bmatrix}B_n^T P_\infty(t)\\ B_n^T P_2(t)\end{bmatrix}]E(t)\\ &\quad -[\rho\Lambda - \rho^{-1}B_n^T P_\infty E]^T \times[\rho\Lambda - \rho^{-1}B_n^T P_\infty E] + \rho^2\Lambda^T\Lambda\end{aligned} \tag{109}$$

where $P_2(t)$ and P_∞(t) are symmetric positive definite solutions of the coupled non-linear differential equations in (100) and (101). Using the differential equation in (101), one can obtain

$$\dot{V}(E,\widetilde{\Phi},\widetilde{\mu},\widetilde{\sigma},\widetilde{b},\widetilde{c},t) = -E^T(t)Q_\infty(t)E(t) + \rho^2\widetilde{\Lambda}^T\widetilde{\Lambda} \tag{110}$$

Integrating (122) from $t=0$ to $t=T$ yields

$$\begin{aligned}&\int_0^T (E^T(t)Q_\infty(t)E(t)dt\\ &\le E^T(0)P_\infty(0)E(0) + \frac{1}{\eta_\Phi}\widetilde{\Phi}^T(0)\widetilde{\Phi}(0) + \frac{1}{\eta_\mu}\widetilde{\mu}^T(0)\widetilde{\mu}(0)\\ &\quad + \frac{1}{\eta_\sigma}\widetilde{\sigma}^T(0)\widetilde{\sigma}(0) + \frac{1}{\eta_b}\widetilde{b}^T(0)\widetilde{b}(0)\\ &\quad + \frac{1}{\eta_c}\widetilde{c}^T(0)\widetilde{c}(0) + \rho^2\int_0^T\widetilde{\Lambda}^T(t)\widetilde{\Lambda}(t)dt\end{aligned} \tag{111}$$

Therefore the $\mathcal{H}_\infty$ control performance is achieved with a prescribed attenuation level ρ^2 and the tracking error $E(t)$ and the estimation error $\widetilde{\Theta}$ in the error dynamic (96) are all bounded.

V. Experimental Results of the Two-Axis Motion Control System

In order to investigate the effectiveness of the proposed tracking control scheme, the simulation and experimentation of the proposed control schemes are carried out using Matlab/Simulink package based on the control system shown in Figs. 1 and 3. A DSP control board dSPACE DS1104, which is based on an MPC8240 64-bit floating-point processor and TMS320F240 DSP, is installed in the control computer The sampling rate is chosen as 200μs and hence, the carrier frequency of the PWM inverter is 5 kHz. The control interval of the motion control loop is set at 1 ms. The current-regulated PWM VSI is implemented using Mitsubishi intelligent power module (IPM) using IGBTs with rating of 50A, 1200V and a switching frequency of 15 kHz and driven by a six Semikron IGBT drivers.

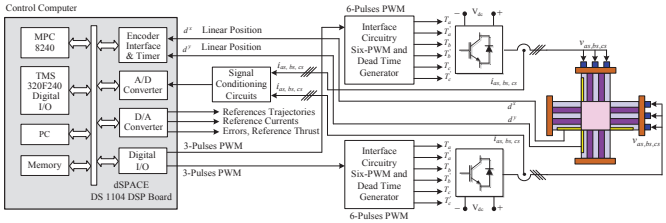

Fig. 3. DSP-based IATCS for two-axis motion control system

A. Experimental Results

To verify the performance of the proposed control schemes applied to the two-axis motion control system in practical applications, some experimental results are introduced. The experimental results of the dynamic performance for the proposed IATCS based on the mixed $\mathcal{H}_2/\mathcal{H}_\infty$ approach using SORFWNN due to circular and polygon reference contours are predicted in Figs. 4 and 5, respectively. First, the IATCS is applied to control the two-axis motion control system. The tracking responses of the X-Y table, the control efforts, and the tracking errors of X-axis and Y-axis due to the circular contour at Case (1) of parameter uncertainties are depicted in Fig. 4(a). Moreover, the tracking responses of the X-Y table, the control efforts, and the tracking errors of X-axis and *y*-axis due to circular contour at Case (2) of parameter uncertainties are illustrated in Fig. 4(b). Second, the proposed IATCS is applied to control the two-axis motion control system with polygon reference contour. The tracking responses of the X-Y table, the control efforts, and the tracking errors of X-axis and Y-axis due to the polygon contour at Case (1) of parameter uncertainness are shown in Fig. 5(a). Moreover, the tracking responses of the X-Y table, the control efforts, and the tracking errors of X-axis and Y-axis due to polygon contour at Case (2) of parameter uncertainness are illustrated in Figs. 5(b). From the experimental results, good tracking responses can be achieved at both cases of parameter variations. Furthermore, robust control characteristics can be obtained with regard to parameter variation. Therefore, the proposed IATCS based on the mixed $\mathcal{H}_2/\mathcal{H}_\infty$ approach using SORFWNN is more suitable to control the two-axis X-Y table when uncertainties occur. It is obvious that the performance of the two-axis motion control system using the IATCS is improved greatly. Thus, it can be verified that the proposed IATC can satisfy the accuracy requirements and is more suitable in the tracking control of the two-axis motion control system for practical applications.

B. Performance Measures

To measure the performance of the servo drive, the maximum tracking error, TE_{max}, the average tracking error, TE_{mean} and the standard deviation of the tracking error, T_{sd}, are defined as follows:

$$TE_{\max} = \max_k \sqrt{T_x(k)^2 + T_y(k)^2} \tag{112}$$

$$TE_{mean} = \sum_{k=1}^{n}\frac{T(k)}{n} \tag{113}$$

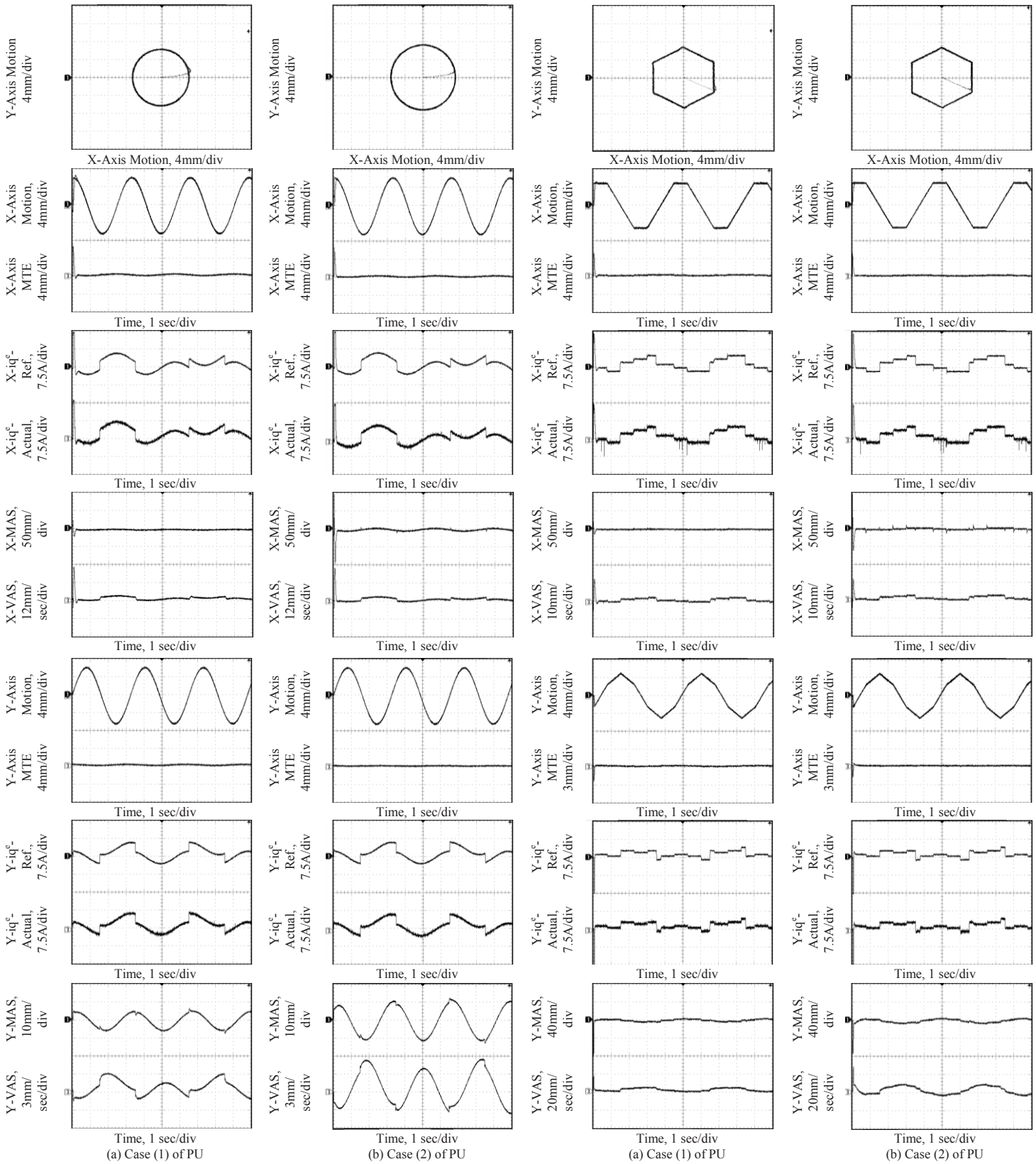

(a) Case (1) of PU (b) Case (2) of PU (a) Case (1) of PU (b) Case (2) of PU

Fig. 4. Experimental results of the dynamic response for the two-axis motion control system with the proposed IATCS based on the mixed $\mathcal{H}_2/\mathcal{H}_\infty$ approach using SORFWNN due to circular contour

Fig. 5. Experimental results of the dynamic response for the two-axis motion control system with the proposed IATCS based on the mixed $\mathcal{H}_2/\mathcal{H}_\infty$ approach using SORFWNN due to polygon contour

$$TE_{sd} = \sqrt{\sum_{k=1}^{n} \frac{(T(k) - T_{mean})^2}{n}} \quad (114)$$

$$T(k) = \sqrt{T_x(k)^2 + T_y(k)^2} \quad (115)$$

where $T_i(k) = [d_i^m(k) - d_i(k)], \quad i = x, y$.

To show the improvement of the control performance of the proposed IATCS, the ideal control system shown in (75) and the fuzzy-wavelet-neural-network controller (FWNNC) are also adopted in the experimentation to control the X-Y table for comparison. To further investigate the improvement of the proposed IATCS, the performance measures of the ideal controller (IC) and FWNNC at the nominal condition and the parameter variation condition are compared and summarized in Tables (I-VI), which include the maximum tracking errors, average tracking errors and the standard deviation of the tracking errors at the two cases of parameters uncertainties. In addition, Tables (VII-X) illustrate the percentage reductions in the tracking errors for both IATCS and FWNNC with respect to ideal control scheme at the same operating conditions. From these results, one can easily observe that high values of TE_{max}, TE_{mean} and TE_{sd} have been successfully reduced by the proposed IATCS. Therefore, the IATCS possesses the best robust control characteristics and can control the two-axis motion control system effectively.

TABLE I
PERFORMANCE MEASURES OF THE IDEAL CONTROLLER AT CASE (1) OF PU FOR THE TWO-AXIS MOTION CONTROL SYSTEM

Contour Type	Tracking Errors (μm)		
	Maximum	Average	S.D.
Circular Contour	85.18	74.32	59.97
Polygon Contour	80.77	70.89	52.86

TABLE II
PERFORMANCE MEASURES OF THE IDEAL CONTROLLER AT CASE (2) OF PU FOR THE TWO-AXIS MOTION CONTROL SYSTEM

Contour Type	Tracking Errors (μm)		
	Maximum	Average	S.D.
Circular Contour	89.13	77.65	63.15
Polygon Contour	83.97	74.56	54.99

TABLE III
PERFORMANCE MEASURES OF THE FWNN CONTROLLER AT CASE (1) OF PU FOR THE TWO-AXIS MOTION CONTROL SYSTEM

Contour Type	Tracking Errors (μm)		
	Maximum	Average	S.D.
Circular Contour	62.90	51.24	45.39
Polygon Contour	60.26	28.67	19.38

TABLE IV
PERFORMANCE MEASURES OF THE FWNN CONTROLLER AT CASE (2) OF PU FOR THE TWO-AXIS MOTION CONTROL SYSTEM

Contour Type	Tracking Errors (μm)		
	Maximum	Average	S.D.
Circular Contour	68.23	55.11	47.37
Polygon Contour	63.14	32.58	17.85

TABLE V
PERFORMANCE MEASURES OF THE IATCS CONTROLLER AT CASE (1) OF PU FOR THE TWO-AXIS MOTION CONTROL SYSTEM

Contour Type	Tracking Errors (μm)		
	Maximum	Average	S.D.
Circular Contour	16.11	12.59	7.79
Polygon Contour	18.69	10.36	5.74

TABLE VI
PERFORMANCE MEASURES OF THE IATCS CONTROLLER AT CASE (2) OF PU FOR THE TWO-AXIS MOTION CONTROL SYSTEM

Contour Type	Tracking Errors (μm)		
	Maximum	Average	S.D.
Circular Contour	18.31	14.32	8.17
Polygon Contour	21.65	11.28	6.94

TABLE VII
TRACKING ERRORS REDUCTION OF THE FWNNC AT CASE (1) OF PU WITH RESPECT TO IC FOR THE TWO-AXIS MOTION CONTROL SYSTEM

Contour Type	Tracking Errors Reduction (%)		
	Maximum	Average	S.D.
Circular Contour	26.16	31.05	24.31
Polygon Contour	25.39	59.56	63.33

TABLE VIII
TRACKING ERRORS REDUCTION OF THE FWNNC AT CASE (2) OF PU WITH RESPECT TO IC FOR THE TWO-AXIS MOTION CONTROL SYSTEM

Contour Type	Tracking Errors Reduction (%)		
	Maximum	Average	S.D.
Circular Contour	30.18	29.03	24.99
Polygon Contour	24.81	56.30	67.54

TABLE IX
TRACKING ERRORS REDUCTION OF THE IATCS AT CASE (1) OF PU WITH RESPECT TO IC FOR THE TWO-AXIS MOTION CONTROL SYSTEM

Contour Type	Tracking Errors Reduction (%)		
	Maximum	Average	S.D.
Circular Contour	81.09	83.06	87.01
Polygon Contour	76.86	85.39	89.14

TABLE X
TRACKING ERRORS REDUCTION OF THE IATCS AT CASE (2) OF PU WITH RESPECT TO IC FOR THE TWO-AXIS MOTION CONTROL SYSTEM

Contour Type	Tracking Errors Reduction (%)		
	Maximum	Average	S.D.
Circular Contour	79.46	81.56	87.06
Polygon Contour	74.22	84.87	87.38

VI. CONCLUSION

This paper proposed an IATCS based on the mixed $\mathcal{H}_2/\mathcal{H}_\infty$ approach using self-organizing recurrent fuzzy-wavelet-neural-network (SORFWNN) for achieving high precision performance of a two-axis motion control system which guarantees the robustness in the presence of parameter uncertainties, external disturbances, cross-coupled interference and frictional force. The proposed IATCS comprises an SORFWNN controller, a robust controller and a mixed $\mathcal{H}_2/\mathcal{H}_\infty$ adaptive tracking controller. The SORFWNNC is used as the main tracking controller to approximate an unknown nonlinear dynamic function which includes the lumped parameter uncertainty and the robust controller is designed to deal with the approximation error, optimal parameter vectors and higher order terms in Taylor series. Whereas the mixed $\mathcal{H}_2/\mathcal{H}_\infty$ controller is designed such that the

quadratic cost function is minimized and the worst case effect of the unknown nonlinear dynamic function on the tracking error must be attenuated below a desired attenuation level. The online adaptive control laws are derived based on Lyapunov theorem and the mixed $\mathcal{H}_2/\mathcal{H}_\infty$ tracking performance so that the stability of the IATCS can be guaranteed. The experimental results due to reference contour trajectories confirm that the proposed IATCS grants robust performance and precise dynamic response regardless of parameter uncertainties and external disturbances.

REFERENCES

[1] K.K. Tan, T.H. Lee, H.F. Dou, and S.N. Huang, *Precision Motion Control: Design and Implementation (Advances in Industrial Control)*. London, U.K.: Springer-Verlag, 2001.

[2] T.C. Chiu and M. Tomizuka, "Coordinated position control of multi-axis mechanical system," *Trans. ASME, J. Dyn. Syst. Meas. Control*, vol. 120, no. 3, pp. 389–393, 1998.

[3] M. H.Smith, A. M. Annaswamy, H. Slocum, *Adaptive control strategies for a precision machine tool axis*. Precis Eng 1995.

[4] S. Goto, M. Nakamura, and N. Kyura, "Accurate contour control of mechatronic servo systems using gaussian networks," *IEEE Trans. Ind. Electron.*, vol. 43, no. 4, pp. 469-476, 1996.

[5] Jacek F. Gieras, Zbigniew J. Piech, Bronislaw Tomczuk, *Linear Synchronous Motors: Transportation and Automation Systems*, CRC Press, Second Edition, 2011.

[6] S. A. Nasar and I. Boldea, *Linear Electric Motors: Theory, Design, and Practical Applications*. Englewood Cliffs, NJ: Prentice-Hall, 1987.

[7] I. Boldea and S. A. Nasar, *Linear Electric Actuators and Generators*. Cambridge, U.K.: Cambridge Univ. Press, 1997.

[8] Y. G. Leu, T. T. Lee and W. Y. Wang, "On-line tuning of fuzzy-neural network for adaptive control of nonlinear dynamical systems," *IEEE Trans. Syst., Man, Cybern*., vol. 27, no. 6, , pp. 1034-1043, 1997.

[9] Y. M. Park, M. S. Choi, and K. Y. Lee, "An optimal tracking neurocontroller for nonlinear dynamic systems," *IEEE Trans. Neural Networks*, vol. 7, no. 5, pp. 1099-1110, 1996.

[10] K. T. Tanaka and H. O. Wang, *Fuzzy Control Systems Design and Analysis*, New York: Wiley, 2001.

[11] R. H. Abiyev, O. Kaynak, "Fuzzy Wavelet Neural Networks for Identification and Control of Dynamic Plants—A Novel Structure and a Comparative Study," *IEEE Trans. on Industrial Electronics*, vol. 55, no. 8, pp. 3133-3140, 2008.

[12] S. Yilmaz and Y. Oysal, "Fuzzy wavelet neural network models for prediction and identification of dynamical systems," *IEEE Trans. Neural Netw*., vol. 21, no. 10, pp. 1599-1609, 2010.

[13] CH Lu, "Wavelet fuzzy neural networks model for identification and predictive control of dynamical systems," *IEEE Trans. Ind. Electron*., vol. 58, no. 7, pp. 3046–3058, 2011.

[14] C. F. Hsu, "Adaptive fuzzy wavelet neural controller design for chaos synchronization," *Expert. Syst. with Appli. an International Journal*, vol. 38, no. 8, pp. 10475-10483, 2011.

[15] M. Davanipoor M. Zekri and F. Sheikholeslam, "Fuzzy wavelet neural network with an accelerated hybrid learning algorithm," *IEEE Trans. Fuzzy Syst*., vol. 20, no. 3, pp. 463-470, 2012.

[16] Wei-Hann Yao, Pi-Cheng Tung, Chyun-Chau Fuh, and Fu-Chu Chou, "Suppression of Hunting in an ILPMSM Driver System Using Hunting Compensator," *IEEE Trans. on Industrial Electronics*, vol. 60, no. 7, pp. 2586-2594, July 2013.

[17] Kwanghyun Cho, Jonghwa Kim, Seibum Ben Choi, and Sehoon Oh, "A High-Precision Motion Control Based on a Periodic Adaptive Disturbance Observer in a PMLSM," *IEEE/ASME Transactions on Mechatronics*, Digital Object Identifier 10.1109/TMECH.2014.2365996, to be published.

[18] Young-Doo Yoon, Eunsoo Jung and Seung-Ki Sul, "Application of a Disturbance Observer for a Relative Position Control System," *IEEE Transactions on Industry Applications*, vol. 46, no. 2, pp. 849-856, March/April 2010.

[19] Faa-Jeng Lin, Kuo-Kai Shyu, Chih-Hong Lin, "Incremental Motion Control of Linear Synchronous Motor," *IEEE Transactions on Aerospace and Electronic Systems*, vol. 38, no. 3, pp. 1011-1022, July 2002.

[20] Yi-Sheng Huang and Cheng-Chung Sung, "Function-Based Controller for Linear Motor Control Systems," *IEEE Transactions on Industrial Electronics*, vol. 57, no. 3, pp. 1096-1105, March 2010.

[21] Mei-Yung Chen and Jian-Shiun Lu, "Application of Adaptive Variable Speed Back-Stepping Sliding Mode Controller for PMLSM Position Control," *Journal of Marine Science and Technology*, vol. 22, no. 3, pp. 392-403, 2014.

[22] Kinjiro Yoshida, M. El-Nemr and Fayez F. M. El-Sousy, "Propulsion and Levitation H^∞ Optimal Control of Underwater Linear Motor Vehicle ME02," *WSEAS Transactions on Systems*, Issue 7, Vol. 4, pp. 1009-1016, July, 2005.

[23] F.-J. Lin, L.-T. Teng, H. Chu, "Modified Elman neural network controller with improved particle swarm optimization for linear synchronous motor drive," *IET Electr. Power Appl*, vol. 2, no. 3, pp. 201–214., 2008.

[24] F.-J. Lin, P.-H. Shen, P.-H. Chou and S.-L. Yang, "TSK-type recurrent fuzzy network for DSP-based permanent-magnet linear synchronous motor servo drive," *IEE Proc.-Electr. Power Appl*., vol. 153, no. 6, pp. 921-931, November 2006.

[25] Chaio-Shiung Chen, Wen-Chi Lin, "Self-adaptive interval type-2 neural fuzzy network control for PMLSM drives," *Expert Systems with Applications,* vol. 38, pp. 14679–14689, 2011.

[26] Faa-Jeng Lin, Li-Tao Teng, and Hen Chu, "A Robust Recurrent Wavelet Neural Network Controller with Improved Particle Swarm Optimization for Linear Synchronous Motor Drive," *IEEE Transactions on Power Electronics*, vol. 23, no. 6, pp. 3067-3078, November 2008.

[27] F. J. Lin, P. H. Shieh and P. H. Shen, "Robust recurrent-neural network sliding-mode control for the X-Y table of a CNC machine," *IEE Proc. Control Theory Application,* vol. 153, no. 1, pp. 111-123, 2006.

[28] F.-J. Lin, P.-H. Chou, Y.-S. Kung, "Robust fuzzy neural network controller with nonlinear disturbance observer for two-axis motion control system," *IET Control Theory Appl*., vol. 2, no. 2, pp. 151–167, 2008.

[29] Faa-Jeng Lin, and Po-Hung Shen, "Robust Fuzzy Neural Network Sliding-Mode Control for Two-Axis Motion Control System," *IEEE Transactions on Industrial Electronics*, vol. 53, no. 4, pp. 1209-1225, August 2006.

[30] Faa-Jeng Lin, Po-Huan Chou, Chin-Sheng Chen, and Yu-Sheng Lin, "DSP-Based Cross-Coupled Synchronous Control for Dual Linear Motors via Intelligent Complementary sliding Mode Control," *IEEE Transactions on Industrial Electronics*, vol. 59, no. 2, pp. 1061-, 1072, February 2012.

[31] F.-J. Lin H.-J. Hsieh P.-H. Chou, "Tracking control of a two-axis motion system via a filtering-type sliding-mode control with radial basis function network," *IET Control Theory Appl,.* vol. 4, no. 4, pp. 655–671, 2010.

[32] Zhou, K., K. Glover, B. Bodenheimer, and J. Doyle, "Mixed H_2 and H_∞ Performance Objectives I: Robust Performance Analysis," *IEEE Trans. Automat. Contr*., vol. 39, pp. 1564-1574, 1994.

[33] Doyle, J., K. Zhou, K. Glover, and B. Bodenheimer, "Mixed H_2 and H_∞ Performance Objectives II: Optimal Control," *IEEE Trans. Automat. Contr*., vol. 39, pp. 1575-1587, 1994.

[34] Tseng, C.S. and B.S. Chen, "A Mixed H_2/H_∞ Adaptive Tracking Control for Constrained Nonholonomic Systems," *Automatica*, vol. 39, pp. 1011-1018, 2003.

[35] Chung-Shi Tseng, "Mixed H_2/H_∞ Adaptive Tracking Control Design For Uncertain Constrained Robots," *Asian Journal of Control*, vol. 7, no. 3, pp. 296-309, September 2005.

[36] J. J. E. Slotine and W. Li, *Applied Nonlinear Control*, Prentice-Hall, New Jersey, 1991.

[37] K. J. Astrom and B. Wittenmark, *Adaptive Control*, Addison-Wesley, New York, 1995.

[38] Anderson, B. D. O. and J. B. Moore, *Optimal Control*: *Linear Quadratic Methods*, Prentice Hall, Englewood Cliffs, NJ, 1990.